14th Australasian Fluid Mechanics Conference
Adelaide University, Adelaide, Australia
10-14 December 2001

Interpretation of Space-time Velocity Correlations in Wall Turbulence

A. K. Mesbah Uddin*, I. Marusic and P. K. Subbareddy

Department of Aerospace Engineering & Mechanics
University of Minnesota, Minneapolis, MN 55455, USA

Abstract

Two point space-time correlations of velocity fluctuations have long been viewed as containing a wealth of information about the geometric and statistical structure of eddies in turbulent flows. In this paper, an attempt is made to interpret these measurements in light of Townsend's attached eddy hypothesis. Both numerical (DNS) and experimental data are considered. The experiments were carried out at two different Reynolds numbers in order to interpret the Reynolds number effects in terms of eddy geometry. The DNS data set comes from the channel flow simulation of Moser, Kim & Mansour[5]. A simulation based on the attached eddy hypothesis tests a conjecture for certain geometric and dynamic properties of the constituent eddies, by comparing the statistics gathered from experiment and DNS.

Introduction

Two point space-time correlations of velocity have been recognized as a potential tool for the eduction of the organized events or the *coherent structures*. While various opinions exist as to the exact definition of *coherent structures* and the details of their geometric, kinematic and dynamic characteristics, the prevailing consensus is that coherent structures play a dominant role in transport phenomena in turbulent flows. In this paper various aspects of two-point velocity correlation measurements are examined in light of the attached eddy model of wall turbulence, first proposed by Townsend[10] and, later realized into a phenomenological model by Perry & Chong[7]. Since then, this model has been scrutinized and refined by Perry & coworkers ([6, 8]) and the model has been found to be successful in providing a framework in which to interpret the mean statistics in wall turbulence. However, this work was primarily confined to single point statistics like mean velocity, Reynolds stresses and spectra. The major aim of this paper is to interpret two point statistics in the spirit of the attached eddy model.

Starting from the equations of motion, Theodorsen[9], with some intuitive arguments, proposed that a turbulent shear flow consists of *horseshoe-vortices* inclined in the flow-direction at an average angle of 45^0. These ideas are consistent with the attached eddy model of Townsend[10] where a turbulent boundary layer is viewed as being composed of a range of geometrically similar (*attached*) eddies originating from the wall, with representative lengths scaling with the distance from the wall. Later, Head & Bandyopadhyay[3] showed by very convincing flow-visualization studies with smoke that a turbulent boundary layer appears to consist of a 'forest' of hairpin vortices which lean in the downstream direction at approximately 45^0. These vortices may loosely be termed (*attached*) *eddies* or simply *eddies*. Recent studies by Adrian and coworkers using high resolution planar PIV measurements ([2, 1]) have revealed that the boundary layer is thickly populated with hairpin vortices which appear in groups (*packets*). Adrian, Meinhart & Tomkins[2] showed that the structural information contained in the two-point correlation can be associated with the presence of hairpin vortex packets. In spite of minor differences in the details of the interpretation, this can be regarded as the most convincing experimental evidence in support of the attached eddy model. In a complementary computational study, Marusic[4] showed that by incorporating the scenario of packets into the attached eddy model, some temporal statistics observed in a boundary layer can be validated for the region of the flow where the logarithmic law of the wall holds. In this paper experimental and computational investigations will be presented in an attempt to explain the characteristics of various aspects of two point correlation measurements, including the Reynolds number dependence of these statistics and the geometric structure of the eddies. The focus of the study will be in the outer region of the flow, defined here tentatively as the outer 80% of the boundary layer thickness.

The Experiment

In this paper, we define x, y and z as the stream-wise, span-wise and wall-normal directions respectively; while the fluctuating velocities in these directions are denoted by u, v and w. Any length scale ℓ is normalized by the boundary layer thickness δ_c, if not otherwise stated, and denoted as $\ell^* \equiv \ell/\delta_c$. The experiment was carried out in a nominally zero pressure gradient, open return, blower type wind tunnel having a working section of 940 mm $\times$ 388 mm and a length of 4400 mm, with two normal hot-wire sensors as shown schematically in figure 1. The lower probe will be referred to as the probe A, and the upper one as probe B. For all measurements the stream-wise separation between the probes (Δx^*) was kept at zero, while various wall normal separations (Δz^*) were used. Two flow cases with $Re_\tau \equiv u_\tau \delta_c/\nu$ equal to 1655 and 4705 were considered. Here u_τ is the friction velocity and ν is the kinematic viscosity. With reference to figure 1, the coefficient of two-point space-time normalized cross-correlation $\mathcal{R}_{\mathcal{AB}}$ of the fluctuating velocities at $\mathbf{A}(x_A^*, y_A^*, z_A^*, t)$ and $\mathbf{B}(x_A^* + \Delta x^*, y_A^* + \Delta y^*, z_A^* + \Delta z^*, t + \tau)$, can be written as

$$\mathcal{R}_{AB}[x_A^*, y_A^*, z_A^*, \Delta x^*, \Delta y^*, \Delta z^*, \tau] = \frac{\overline{u_A\, u_B}}{\sqrt{\overline{u_A^2}}\,\sqrt{\overline{u_B^2}}} \quad (1)$$

where u_A and u_B represent the fluctuating components of the stream-wise velocities at $\mathbf{A}$ and $\mathbf{B}$ respectively, τ represents the time-shift parameter and overbars denote ensemble time averages. Although the use of Taylor's hypothesis in flows with strong shear has been the issue of much debate, Uddin, Perry & Marusic[11] showed that when Taylor's hypothesis is used in transforming a

*Present Address: Department of Engineering, University of Tennessee at Martin, TN 38238, USA

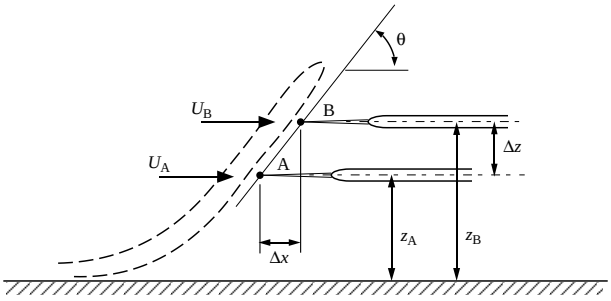

Figure 1: Schematic of experiment and definition of the terms.

temporal-shift τ to a spatial-shift Δx in two-point cross-correlation measurements, an inappreciable error is encountered. Now using Taylor's hypothesis, and choosing the position **A** as the origin of the coordinate system, with Δy^*=0 always, we can write (1) as:

$$R_{AB}[\xi, \Delta z^*] = \frac{\overline{u_A\, u_B}}{\sqrt{\overline{u_A^2}}\,\sqrt{\overline{u_B^2}}}. \qquad (2)$$

The non-dimensional parameter ξ can be defined, in terms of U_c, the convection velocity, and δ_c, as

$$\xi \;=\; \Delta x^* \;-\; \frac{\tau U_c}{\delta_c}. \qquad (3)$$

For convenience, let ξ_0 denote the special case when $\tau = 0$, i.e. $\xi_0 = \Delta x^*$. Note that for all results to follow, a constant convection velocity equal to 82% of the mean free-stream velocity is used (as suggested by Uddin *et al.*[11]).

The Attached Eddy Computation

In general, the induced stream-wise velocity field, U, due to a representative eddy of scale δ and its image in the wall can be written as

$$\frac{U}{U_0} = f[\frac{x}{\delta}, \frac{y}{\delta}, \frac{z}{\delta}] \qquad (4)$$

where U_0 is the characteristic velocity scale. This velocity field can be computed using the Biot-Savart integral. A Gaussian distribution of vorticity within the core of the vortex filaments is assumed. Let $\psi_A[k_1\delta, y/\delta, z/\delta]$ and $\psi_B[k_1\delta, y/\delta, z/\delta]$ denote the one dimensional Fourier transform (in the stream-wise direction) of the fluctuating components of the velocity functions f_A and f_B at A and B respectively. Then, following the analysis given by Marusic[4], the normalized correlation R_{AB} can be written as:

$$R_{AB}[\xi_0, \Delta z^*] = \frac{\mathcal{R}'_{AB}[\xi_0, \Delta z^*]}{\sqrt{\mathcal{R}'_{AA}[0,0]\;\mathcal{R}'_{BB}[0,0]}} \qquad (5)$$

where $\mathcal{R}'_{AB}$ is defined as

$$\mathcal{R}'_{AB}[\xi_0, \Delta z^*] \;=\; \tfrac{U_0^2}{\lambda_x \lambda_y} \int_{-\infty}^{\infty}\int_{\delta_1}^{\delta_c}\int_{-\infty}^{\infty} \psi_A^*\, \psi_B\, Q^2[\tfrac{\delta}{\delta_c}] \;\times\; D[\tfrac{\delta}{\delta_c}]\; \tfrac{1}{\delta}\; d(\tfrac{1}{\delta})\, d\delta\, d(k_1\delta) \qquad (6)$$

where the asterisk denotes a complex conjugate, and λ_x and λ_y are geometric constants relating to the random distribution of eddy length scales in the boundary layer. The limits δ_1 and δ_c denote the smallest and the largest

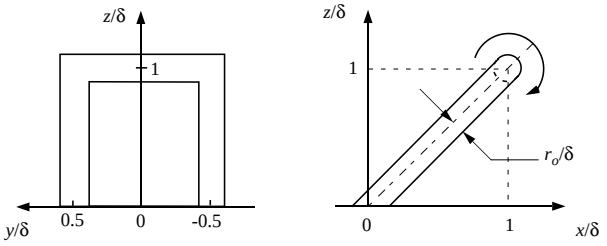

Figure 2: Sketch of a simple Π eddy.

length scales considered which are assumed to be equal to $100\nu/U_\tau$ and the boundary layer thickness respectively. The functions Q and D are weighting functions as defined in Perry & Marusic[6]. Q accounts for the variation of velocity length scale for different δ's, and D accounts for the departure of the eddy length scale distribution p.d.f from a -1 power law and how the p.d.f on the $(x, y, 0)$ surface varies with δ.

Although the numerical simulations were carried out with several eddy geometries, results corresponding to a simple eddy geometry, referred to as a Π-eddy (as in figure 2), will be presented. This simple eddy consists of two predominant types of structure; there are two rods of vorticity inclined at an angle of 45^0 to the downstream direction, referred to as *legs* and one span-wise rod of vorticity, the *head*. Considering the experimental observation that the span-wise correlation of u is confined to $\Delta y \approx \delta_c$ in the outer part of the boundary layer, the span-wise extent of the computational domain was conservatively set to 4δ, divided into 100 equally spaced grid points. Near the wall, the experimental span-wise correlation decays to zero even faster. The stream-wise extent of the computational box was set to 20δ with 4096 equally spaced grid points. Based on some preliminary calculations of spectra, Perry & Marusic[6] suggested that this simple shape with $Q^2D = 1$ in (6) may be a good candidate for the representative eddy in a zero-pressure-gradient boundary layer flow.

Results and Discussion

Correlation Profiles

Marusic[4] showed that incorporating the concept of hairpin vortex packets of Adrian *et al.*[1] in the attached eddy model gives a good qualitative prediction of the characteristics of auto-correlation and two-point space-time cross-correlation near the wall. Complementary to this, our analysis on this occasion will be limited to the outer region of the boundary layer beyond where the log-law of the wall holds. Experimental correlation profiles at various z_A^* in the outer part of the boundary layer corresponding to Re_τ=1655 with Δz^*=0.10, 0.15, 0.20, 0.25 and 0.30 are shown in figure 3. An interesting point can be noted by considering the position $z_A^* \approx 0.54$. It can be seen that the profile with Δz^*=0.30 begins to develop a kink which evolves into a negative peak in the R_{AB} profile at z_A^*=0.77 and culminates into a Mexican Hat like appearance. Similar evolution is observed for the profiles corresponding to Δz^*=0.25 and 0.20, though at different z_A^*. But, though the ultimate appearance of all of the profiles at $z_A^* \approx 1$ is more or less identical, this evolution process is not distinct with Δz^*=0.10 and 0.15. The emergence of the negative R_{AB} can be attributed to the existence of a span-wise vortex element (the head) with the probes at A and B being on the

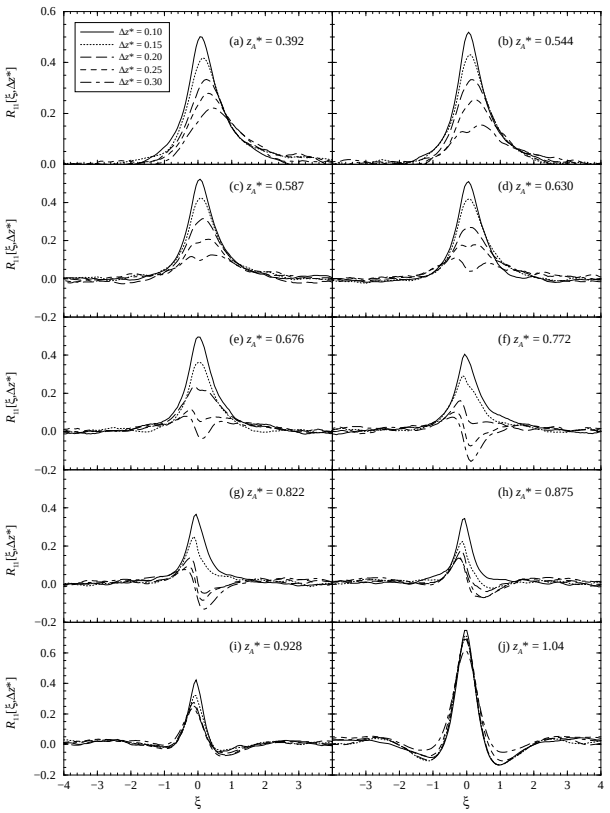

Figure 3: Effect of wall normal separation on the experimental space-time correlation profiles at Re_τ=1655.

lower and upper side of the vortex. This conjecture is supported by the results in figure 4 where R_{AB} profiles computed using the attached eddy model for a range of hierarchy length scales of simple Π-eddies, with r_0^*=0.05 ($r_0^* \equiv r_0/\delta$) and Δz^*=0.15, are shown with the experimental profiles corresponding to Δz^*=0.30. It can be seen that the experimental and computational profiles are going through remarkably similar qualitative evolutions as the probe system is moved towards the edge of the boundary layer. Simulations were carried out with a wide range of r_0^* and Δz^* values and it was found that the detection of the evolution as depicted in figure 4 requires a certain relationship between r_0^* and Δz^*. Based on this and from further evidence to be presented later, it appears that these two experimental and simulation cases represent comparable eddy core-radii to Δz^* ratios. Based on this conclusion, it should be noted that ideally a check is made with a model calculation with Δz^*=0.30 and r_0^*=0.10. However, large core-radii with simple Gaussian distributions of vorticity, combined with large Δz^* values lead to numerical difficulties in the form of singularities. New improved calculation schemes are presently being attempted to overcome this difficulty.

Optimum Correlation

Let ξ_m be the value of ξ where R_{AB} is maximum. This gives $R_{AB}[\xi_m, \Delta z^*]$ which is defined as the optimum correlation. The profiles of the optimal correlation $R_{AB}[\xi_m, \Delta z^*]$ computed using both a single representative eddy length scale and a range of eddy length scales are shown in figure 5. One can see that in case of a single eddy length scale, there is hardly any effect of Δz^* for $z_A^* + \Delta z^* < \delta$, as would be expected (here length scales

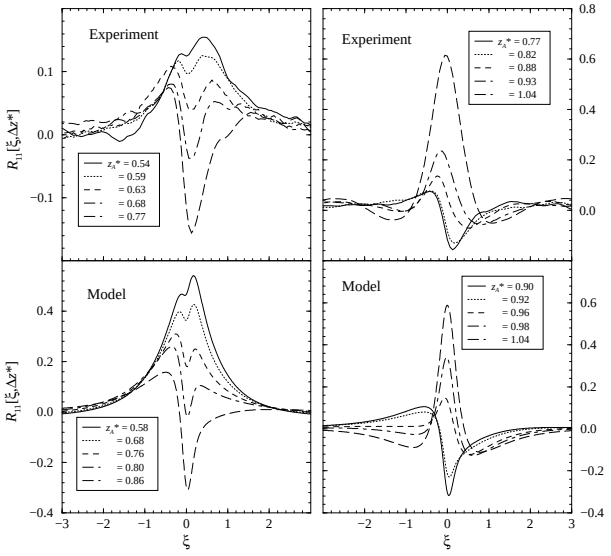

Figure 4: Trends of the experimental and computational correlation profiles in the outer part of the boundary layer. (a) Experiment at Re_τ=1655 with $\Delta z^* = 0.30$. (b) Model with $r_0^* = 0.05$ and $\Delta z^* = 0.15$.

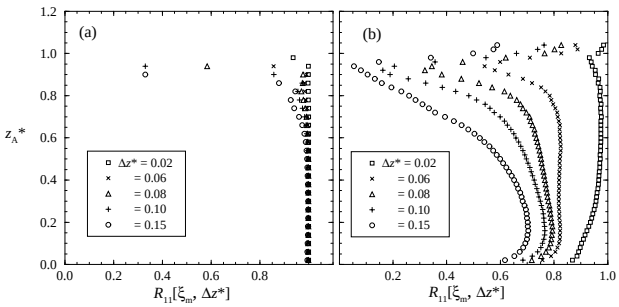

Figure 5: Dependence of the optimal correlation on the wall-normal separation for a given core radius $r_0^* = 0.05$ corresponding to: (a) A single representative structure of one length scale. (b) A range of eddy length scales.

are normalized by the representative eddy length scale δ). However, a significant Δz^* dependence exists when we consider the case with a range of eddy length scales which, in fact, resembles qualitatively the experimental pattern as shown in figure 6. Comparing figures 5(b) and 6(a), we see that for Δz^* equal to 0.10 and 0.15, the optimal R_{AB} exhibits a constant value in the middle portion of the boundary layer. Similar calculations using various r_0^* and Δz^* show that the appearance of this constant value occurs when we have $\Delta z^* \approx r_0^*$. A larger ratio causes the profiles to lean forward towards the abscissa while a smaller ratio causes the opposite effect. The fact that the simulations with a single representative structure do not show any such features indicates that the effect is due to the existence of a range of geometrically similar length scales. The experimental optimum R_{AB} at Re_τ=4705 (figure 6(b)) shows that a similar profile results for a smaller Δz^* of 0.10. Now in line with the earlier observations, this could suggest that the eddies become *skinnier* as the Reynolds number is increased. This trend would not be expected to persist at higher Reynolds numbers, as the ratio should be constant as Re_τ becomes very large, in line with Reynolds number similarity.

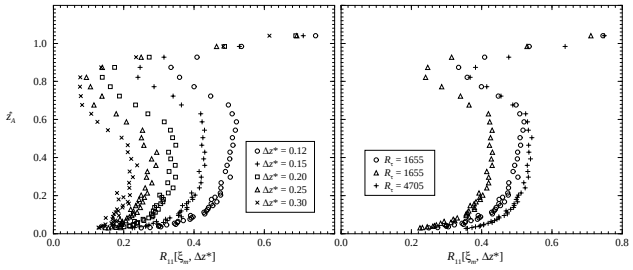

Figure 6: (*a*) Variation of $R_{AB}[\xi_m, \Delta z^*]$ across the boundary layer at Re_τ=1655 for different Δz^*. (*b*) Reynolds number dependence of $R_{AB}[\xi_m, \Delta z^*]$. ◯:$\Delta z^*$=0.10; △:$\Delta z^*$=0.15; +:$\Delta z^*$=0.10.

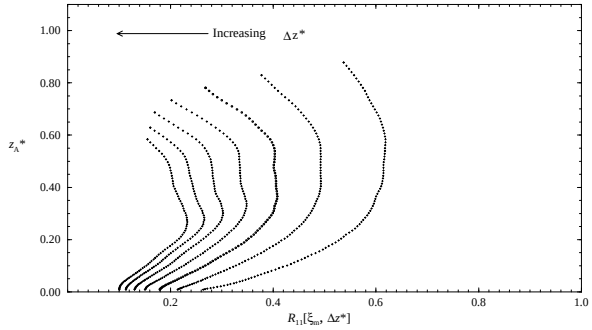

Figure 7: Variation of $R_{AB}[\xi_m, \Delta z^*]$ across the boundary layer for the DNS channel flow data with Δz^*=0.10, 0.15, 0.20, 0.25, 0.30, 0.35 and 0.40.

Optimum correlations calculated from the DNS data are shown in figure 7 corresponding to various wall-normal separations Δz^* of 0.10, 0.15, 0.20, 0.25, 0.30, 0.35 and 0.40. The DNS results are calculated using the channel flow data of Moser, Kim & Mansour[5] corresponding to $Re_\tau \approx$590. The results represent statistics averaged over 74 time-steps. It is obvious from figure 7 that the profiles corresponding to different Δz^* follow the trends as found in the experiment and in the attached eddy simulation results. In this case, the profile corresponding to Δz^*=0.20 shows a considerable region of constant optimum R_{AB} and profiles corresponding to a larger Δz^* than this seem to lean forward while those corresponding to a smaller Δz^* lean backward. Following the earlier arguments it can be conjectured that the non-dimensional eddy core-radius in the DNS case is approximately 0.20. Now considering the Re_τ values of the DNS case this seems to be a plausible value. However, the nature of the optimum correlation profiles near the edge of the layer (for $z_A^* + \Delta z^* \approx 1$) seems to be different from the boundary layer cases (both experiment and simulation). This is expected since the channel flow will not have the intermittent nature of turbulence which will be present in the flat plate boundary layer flow.

Conclusions

Various trends observed in the outer region (beyond the logarithmic region) of a zero pressure gradient boundary layer can be attributed to eddies with geometries which can be approximated by a simple Π structure. The statistics are found to be dependent on the Reynolds number of the flow which seems to affect the core-diameter of the constituent eddies; in a higher Reynolds number flow the eddies seem to be more stretched with a smaller core radius. Subsequently, the postdiction of two-point correlation statistics must take into account the wall-normal separation to eddy core-radius ratio. The two-point statistics in a channel flow showed similar trends except near the edge of the layer.

Acknowledgement

The authors wish to thank Professor Robert Moser, University of Illinois, Urbana-Champagne, for kindly making available the DNS data. Support from the National Science Foundation is gratefully acknowledged.

References

[1] Adrian, R. J., Meinhart, C. D., & Tomkins, C. D. (2000). Vortex organization in the outer region of the turbulent boundary layer. *Journal of Fluid Mechanics* **422**, 1–54.

[2] Christensen, K. T. & Adrian, R. J. (2001). Statistical evidence of hairpin vortex packets in wall turbulence. *Journal of Fluid Mechanics* **431**, 433–443.

[3] Head, M. R. & Bandyopadhyay, P. (1981). New aspects of turbulent boundary-layer structure. *Journal of Fluid Mechanics* **107**, 297–338.

[4] Marusic, I. (2001). On the role of large-scale structures in wall turbulence. *Physics of Fluids* **13**, 735–743.

[5] Moser, R. D., Kim, J. & Mansour, N. N. (1999). Direct numerical simulation of channel flow up to Re_τ=590 *Physics of Fluids* **11**, 943–945.

[6] Perry, A. E. & Marusic, I. (1995). A wall-wake model for the turbulence structure of boundary layers. Part 1. *Journal of Fluid Mechanics* **298**, 361–388.

[7] Perry, A. E. & Chong, M. S. (1982). On the mechanism of wall turbulence. *Journal of Fluid Mechanics* **119**, 173–217.

[8] Perry, A. E., Henbest, S. M & Chong, M. S. (1986). A theoretical and experimental study of wall turbulence. *Journal of Fluid Mechanics* **165**, 163–199.

[9] Theodorsen, T. (1952). Mechanism of turbulence. In *Proc. Second Midwestern Conference on Fluid Mechanics,* The Ohio State University, March 17-19, 1952.

[10] Townsend, A. A. (1956). *The Structure of Turbulent Shear Flow.* Cambridge University Press.

[11] Uddin, A. K. M., Perry, A. E., & Marusic, I. (1997). On the validity of Taylor's hypothesis in wall turbulence. *Journal of Mech. Engg Res. and Dev.* **19-20**, 57–66.